ISSN: 1231-4005
e-ISSN: 2354-0133
DOI: 10.5604/12314005.1213585

ANALYSIS OF THE DETONATION INITIATION POINT POSITION INFLUENCE ON THE CYLINDRICAL FRAGMENTATION WARHEAD EFFECTIVENESS

Robert Panowicz, Marcin Konarzewski, Michał Trypolin

Military University of Technology
Department of Mechanics and Applied Computer Science
Kaliskiego Street 2, 00-908 Warsaw, Poland
tel.: +48 22 683-98-49, fax. +48 22 683-93-55
e-mail: robert.panowicz@wat.edu.pl, marcin.konarzewski@wat.edu.pl

Abstract

The article presents results of the numerical analyses of the fragmentation warhead, which is one of the key elements of the missile used to combat anti-tank missiles. The fragmentation warhead is composed of such elements as outer casing, inner casing, explosive material and fragmentation liner. The fragmentation liner is built from steel spheres or cylinders embedded in epoxy resin. As a result of the explosive material detonation the pressure wave is generated, which affects the liner, causes its fragmentation, and drives each splinter. In order to perform numerical analyses the model of the cylindrical fragmentation warhead with a diameter of 80 millimetres and a length of 100 mm was prepared. The fragmentation liner consists of steel spheres with a diameter of 5 mm. It was assumed in simulation that the detonating material is the plastic explosive C4. The influence of the position of the explosive charge detonation initiation point of the fragmentation warhead on its effectiveness was studied. Effectiveness was evaluated by measuring the maximum speed obtained by the fragments and their spatial distribution. A three-dimensional model of the studied system has been prepared using the MSC Patran software and the numerical analyses were performed using the finite element method with explicit scheme of the time integration implemented in the LS-Dyna solver. To model gas domain Arbitrary Lagrangian-Eulerian (ALE) method was used and interaction between gas and solid body was modelled with FSI coupling.

Keywords: *finite elements method, dynamics, directed fragmentation warheads*

1. Introduction

In order to prevent military objects (such as tanks) from destroying by cumulative missiles different kinds of protection systems are used. The simplest are passive systems like rod or slat armour [3]

Active protection systems are much more sophisticated and generally are consisted of three basic systems:

- the detection system,
- the decision-making system,
- the counter-measure system.

Presented in the article cylindrical fragmentation warhead is a main part of the counter-measure system. The warhead consists of three parts: metallic cover, explosive material and a fragmentation liner. The main task of a warhead is to create a cloud of the fragments, which damage the shaped charge or create short circuit in the approaching anti-tank missile. Thus analyse of parameters which may influence the effectiveness of fragments is very important. In the previous articles authors presented influence of such parameters as outer case material [4] or fragmentation liner material stiffness [6].

The effectiveness of fragments originating from fragmentation warhead is evaluated by measuring the maximum velocity of the fragments and their spatial distribution.

Cylindrical fragmentation warhead is presented in the Fig. 1.

Fig. 1. Cylindrical fragmentation warhead

2. Numerical model

In order to perform numerical analyses a three-dimensional numerical model of the 100 millimetres long cylindrical fragmentation warhead with the diameter of 80 millimetres was prepared. In the discussed model, we can distinguish three main parts: an outer case, a fragmentation liner and an explosive charge. In addition, it was necessary to model an air surrounding the analysed system because numerical analyses were performed with use of the ALE (Arbitrary Lagrangian-Eulerian) method and FSI (fluid-structure interaction) coupling.

The fragmentation liner is composed from the steel spheres having a diameter of 5 millimetres, which were embedded in the epoxy resin. In the numerical model, there are 1296 spheres for which discretization it was necessary to use 54432 solid finite elements.

Bilinear material model was used to describe the material properties of steel balls. In this model, the behaviour of material is defined using points describing the stress and corresponding strains (ES, EPS in the material model keyword). Between each point, the behaviour of the material is considered as linear. There is also possibility to define a failure criterion in the form of maximum strain at the failure – ε_f.

Used material constants for steel balls are presented in the Tab. 1.

Tab. 1 Material constants for the bilinear material model

Parameter	Unit	Value
ρ	kg/mm^3	7.89e-6
E	GPa	210
v	-	0.3
ε_f	-	0.2
EPS1	-	0.02
EPS2	-	0.4
ES1	GPa	0.21
ES2	GPa	0.218

The steel balls are emedeed in the epoxy resin. Due to the fact that their strength is very low in comparison to the other materials used in the cylindrical fragmentation warhead, the Mie-Gruneisen equation was used to describe its behaviour [1]. In the same way air, surrounding the entire system was modelled with only changed density.

$$p = p_0 + \gamma\rho E, \tag{1}$$

where:
p – pressure,
p_0 – initial pressure,
γ – Gruneisen coefficient,
ρ – density,
E – internal energy.

The material constants were taken from the literature [5] and were γ=1.4; ρ=1.185 kg/m^3; p_0=1013 hPa.

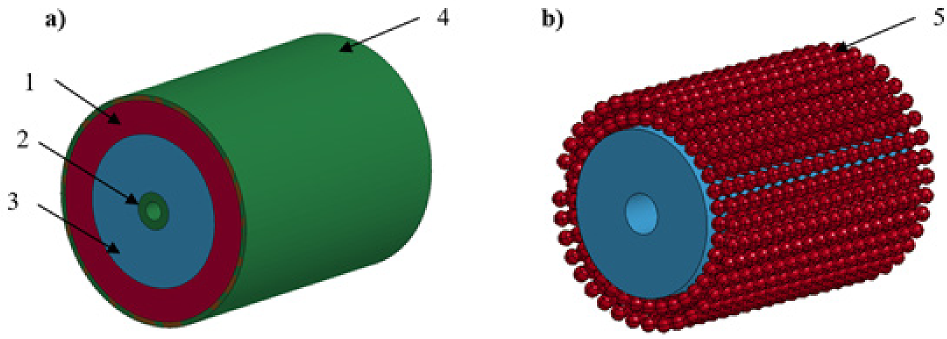

Fig. 2. Numerical model of the cylindrical fragmentation warhead a) entire model b) fragmentation liner, 1 - fragmentation liner, 2 – inner case (optional), 3 – explosive charge, 4 – outer case, 5 – steel balls

The behaviour of the outer case was simulated by using the simplified Johnson-Cook material model [1]. The simplified model, as opposed to the full model, does not take into consideration the influence of thermal effects on the material. The strain rate effect is the same as in the full Johnson-Cook model.

$$\sigma_{flow} = [A + B(\varepsilon^p)^n]\left(1 + Cln\dot{\varepsilon}^{p^*}\right), \tag{2}$$

where:
A, B, C, n, m – material constants,
$\dot{\varepsilon}$ – strain rate.

Tab. 2. Johnson-Cook material constants [9]

Parameter	Unit	Value
ρ	kg/mm^3	7.89e-6
E	GPa	210
v	-	0.3
A	GPa	0.365
B	GPa	0.51
n	-	0.9
C	-	0.0936
ε_f	-	0.3

The detonation process was described using programmed burn model approximations [2], and the behaviour of detonation products was described with the JWL (John, Wilkins, Lee) equation [7]:

$$p = A\left(1 - \frac{\omega}{R_1 V}\right)^{-R_1 V} + B\left(1 - \frac{\omega}{R_2 V}\right)^{-R_2 V} + \omega\rho E\,, \tag{3}$$

where:
$V = \rho_0 / \rho$,

ρ_0 – initial density,
ρ – density of detonation products,
A, B, R_1, R_2, ω – values constant.

The values parameter of the JWL equation is presented in Tab. 3.

Tab. 3. The values constant of the JWL equation for C4 [7]

Parameter	Unit	C4
ρ	kg/mm^3	1.6e-6
D	mm/ms	8000
PCJ	GPa	28
A	GPa	609
B	GPa	12.95
R_1	-	4.5
R_2	-	1.4
ω	-	0.25

3. Numerical analyses

Authors performed analyses of influence of the initial detonation point location on the cylindrical fragmentation warheads fragmentation process effectiveness. For this purpose author prepared four variants of the numerical model (Fig. 3):

- variant A – detonation point located on the left end of the warhead head close to the axis of the charge,
- variant B – detonation point located on the left end of the warhead head far from the axis of the charge,
- variant C – detonation point located in the middle of the warhead head close to the axis of the charge,
- variant D – detonation point located in the middle of the warhead head far from the axis of the charge.

In the every case, authors analysed the speed of the fragments originating from:

- the detonation point and the opposite side of the warhead (in variant A and B),
- the detonation point and the left and right end of the warhead (in variant C and D).

The steel balls were originally located in two layers. Speed was measured for four fragments from every end of the warhead and from every layer (Fig. 4).

In order to maintain readability of the article authors presents in the form of time-velocity graphs only results for the fragments originating from the top layer. Full results are presented in the Tab. 4.

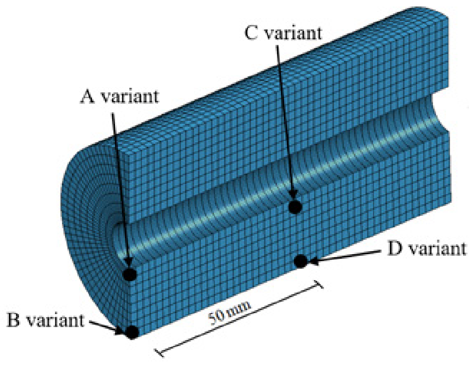

Fig. 3. Prepared variants of the detonation point location (detonation point identified with a dot)

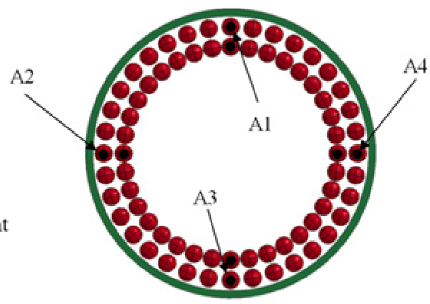

Fig. 4. Initial location of the fragments for which velocity was measured

a) A variant

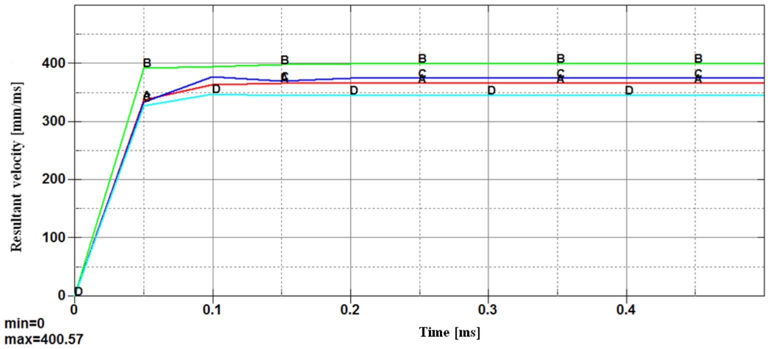

Fig. 5. Time-velocity graph for fragments originating from detonation point – top layer

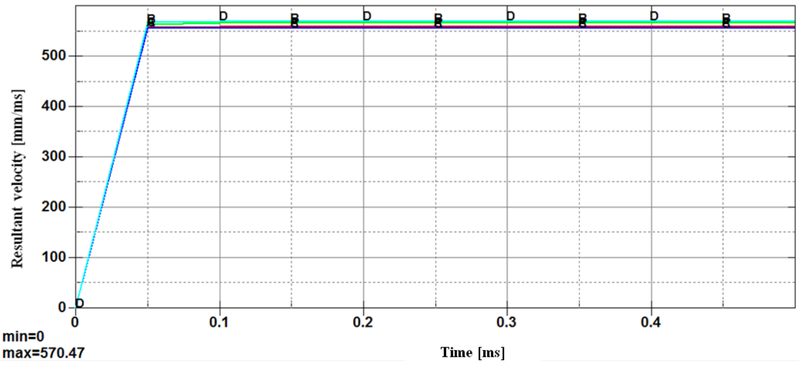

Fig. 6. Time-velocity graph for fragments originating from opposite end – top layer

b) B variant

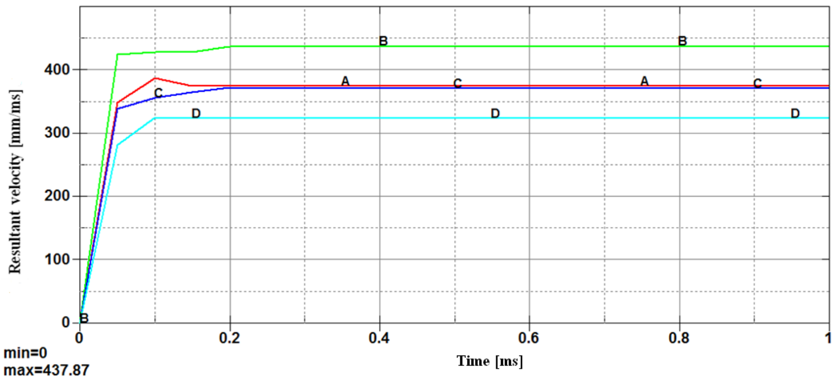

Fig. 7. Time-velocity graph for fragments originating from detonation point – top layer

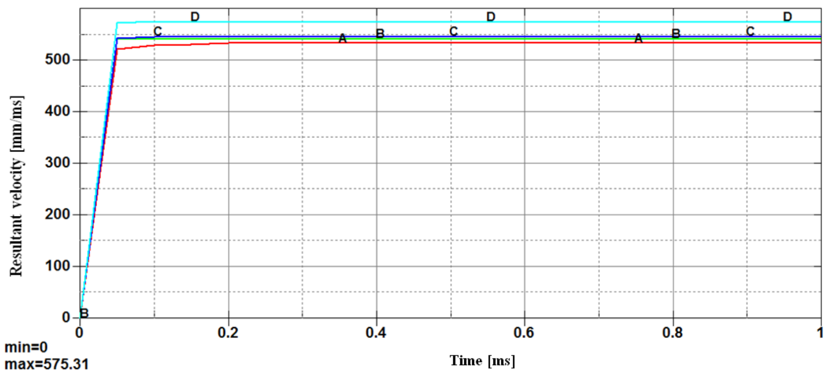

Fig. 8. Time-velocity graph for fragments originating from opposite end – top layer

c) C variant

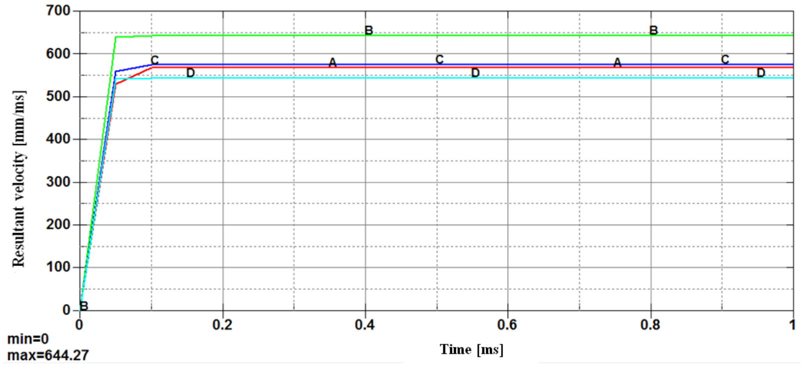

Fig. 9. Time-velocity graph for fragments originating from detonation point ‒ top layer

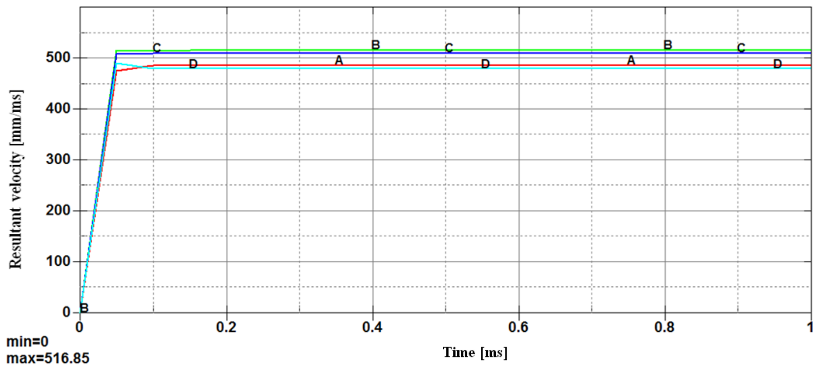

Fig. 10. Time-velocity graph for fragments originating from left end – top layer

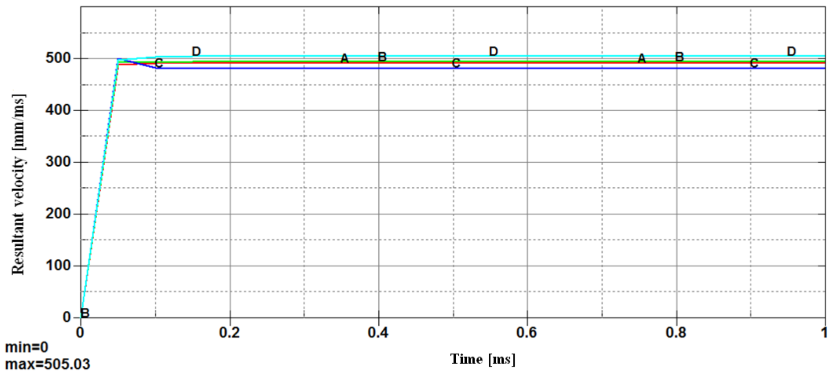

Fig. 11. Time-velocity graph for fragments originating from right end ‒ top layer

d) D variant

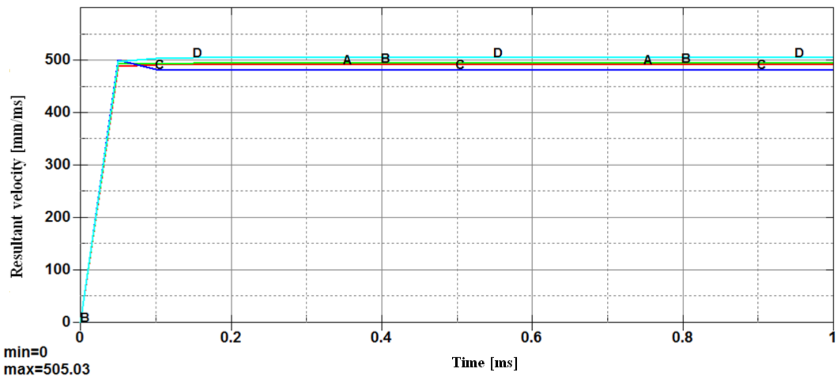

Fig. 12. Time-velocity graph for fragments originating from detonation point ‒ top layer

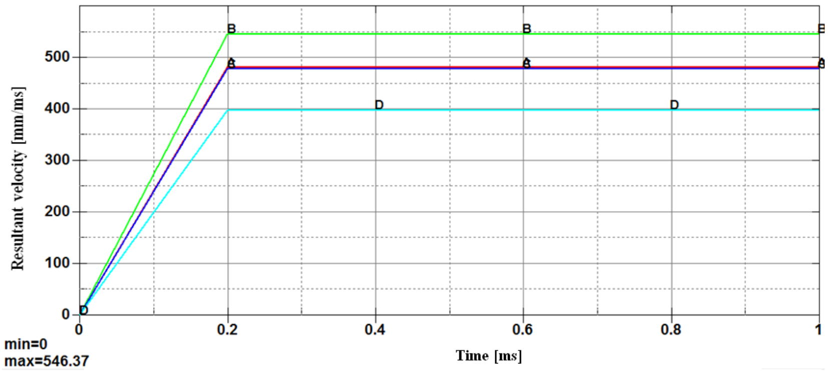

Fig. 13. Time-velocity graph for fragments originating from left end – top layer

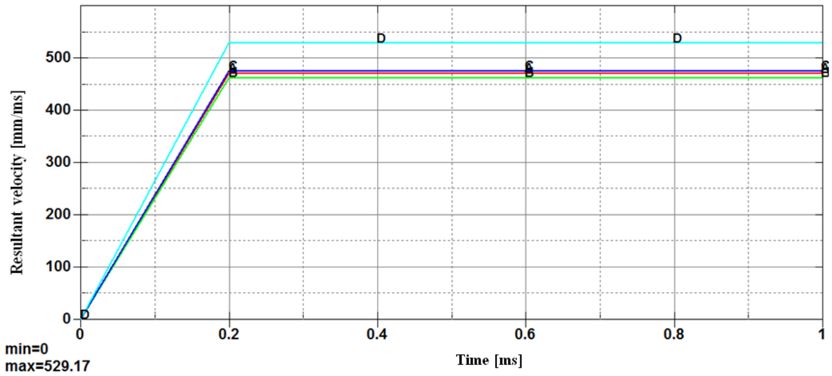

Fig. 14. Time-velocity graph for fragments originating from right end – top layer

Localisation of the detonation point has a very large impact on the effectiveness of the fragmentation process. The greatest values of the fragments velocities were obtained for the cases where the detonation point was located in the middle of the warhead. Comparing the cases where the detonation point is located close to the outer casing (variant B and D) we may observe that the velocity of fragments originating from the detonation point is about 39% higher for the variant where the detonation point was located in the middle of the warhead.

Comparing the cases where the detonation point is located in the middle (variant C and D) but in different distance from the axis of charge, we can also observe difference in the fragments velocity. In this case, the difference is much lower and amounts only 10%.

Tab. 4. The maximum velocity of the fragments

	Layer	A variant [mm/ms]	B variant [mm/ms]	C variant [mm/ms]	D variant [mm/ms]
Detonation point	Top	401	437	644	718
	Bottom	435	459	639	714
Left end	Top	570	575	517	546
	Bottom	547	558	482	516
Right end	Top	-	-	505	529
	Bottom	-	-	469	509

4. Summary

Article present study on the influence of the initial detonation point localisation on the fragmentation process effectiveness. Authors measured maximal velocity for fragments originating from different parts of the fragmentation warhead. The highest values were obtained for detonation point located in the middle of the warhead.

Acknowledgement

The paper is founded from project DOBR-BIO4/031/13249/2013 supported by The National Centre for Research and Development. This support is gratefully acknowledged.

References

[1] Hallquist, J. O., *LS-Dyna Theory Manual*, Livermore Software Technology Corporation, Livermore 2005.

[2] Kapila, A. K., Bdzil, J. B., Stewart, D. S., *On the structure and accuracy of programmed burn*, Combustion Theory and Modelling, Vol. 10, Is. 2, 2006.

[3] Niezgoda, T., Panowicz, R., Sybilski, K., *Model MES pocisku PG-7G: wstępna analiza numeryczna oddziaływania pocisku z przeszkodą*, Mechanik, 83, 7, 2010.

[4] Nowak, J., Panowicz, R., Konarzewski, M., *Influence of destructor case type on separate of fragments in military vehicles active protection system*, Journal of KONES Powertrain and Transport, Vol. 21, No. 1, pp. 183-187, 2014.

[5] Masahiko, O., Yamato, M., Kenji, M., Yukio, K., Shigeru, I., *A Study on Shock Wave Propagation Process in the Smooth Blasting Technique*, 8th International LS-DYNA Conference, Detroit 2004.

[6] Panowicz, R., Nowak, J., Konarzewski, M., Niezgoda, T., *Parametric studies of directed fragmentation warhead used for combat shaped charges,* Engineering Transactions, 63, 2, pp. 181-190, 2015

[7] Włodarczyk, E., *Wstęp do mechaniki wybuchu*, PWN, Warsaw 1994.